JOURNAL OF GEOPHYSICAL RESEARCH: OCEANS, VOL. 118, 1–11, doi:10.1002/jgrc.20399, 2013

A climatology-based quality control procedure for profiling float oxygen data

Yuichiro Takeshita,[1] Todd R. Martz,[1] Kenneth S. Johnson,[2] Josh N. Plant,[2] Denis Gilbert,[3] Stephen C. Riser,[4] Craig Neill,[5] and Bronte Tilbrook[5]

Received 31 March 2013; revised 31 July 2013; accepted 12 September 2013.

[1] Over 450 Argo profiling floats equipped with oxygen sensors have been deployed, but no quality control (QC) protocols have been adopted by the oceanographic community for use by Argo data centers. As a consequence, the growing float oxygen data set as a whole is not readily utilized for many types of biogeochemical studies. Here we present a simple procedure that can be used to correct first-order errors (offset and drift) in profiling float oxygen data by comparing float data to a monthly climatology (World Ocean Atlas 2009). Float specific correction terms for the entire array were calculated. This QC procedure was evaluated by (1) comparing the climatology-derived correction coefficients to those derived from discrete samples for 14 floats and (2) comparing correction coefficients for seven floats that had been calibrated twice prior to deployment (once in the factory and once in-house), with the second calibration ostensibly more accurate than the first. The corrections presented here constrain most float oxygen measurements to better than 3% at the surface.

Citation: Takeshita, Y., T. R. Martz, K. S. Johnson, J. N. Plant, D. Gilbert, S. C. Riser, C. Neill, and B. Tilbrook (2013), A climatology-based quality control procedure for profiling float oxygen data, *J. Geophys. Res. Oceans*, *118*, doi:10.1002/jgrc.20399.

1. Introduction

[2] Profiling floats provide a near-ideal platform for monitoring the seasonal evolution of both physical and chemical processes at the regional, basin, and global scale. The number of oxygen measurements from profiling floats is rapidly growing, with over 450 "Argo Equivalents" deployed with oxygen sensors (of which >150 are currently operating). Data from these autonomous platforms has yielded new insights into oceanic biogeochemical processes [*Martz et al*., 2008; *Riser and Johnson*, 2008; *Whitmire et al*., 2009; *Johnson et al*., 2010; *Kihm and Körtzinger*, 2010; *Juranek et al*., 2011; *Prakash et al*., 2012]. However, the profiling float oxygen data set is underutilized because, unlike temperature (*T*), salinity (*S*), and pressure (*P*) data, dissolved oxygen (O_2) data are not QC'd by the Argo data centers. For example, *T*, *S*, and *P* data are subject to detailed scrutiny by regional experts after an initial automated QC protocol. Salinity data go through further QC by comparison to a climatology derived from ship-based bottle and CTD data [*Wong et al*., 2003; *Bohme and Send*, 2005; *Owens and Wong*, 2009]. With the number of oxygen measurements from the float array growing rapidly, it is important to develop and evaluate new QC procedures for O_2 in order to promote wide use of the profiling float oxygen data set.

[3] Currently, only a handful of oxygen profiling floats have been validated using discrete samples taken at or near the time of deployment, and the vast majority of the profiling float oxygen data are unverified. Although studies have shown that oxygen sensors on profiling floats can produce highly stable data over months to years [*Körtzinger et al*., 2005; *Tengberg et al*., 2006; *Riser and Johnson*, 2008], examples where large discrepancies (up to 40 μM) between profiling floats and discrete water samples taken nearby the float have been reported [*Kobayashi et al*., 2006]. Clearly, a need to QC the oxygen data from profiling floats exists.

[4] Here we present a simple QC procedure for profiling float oxygen data based on comparing float data to a monthly climatology and therefore driving corrected float data toward the climatology. The Argo float oxygen data set from the U.S. Global Ocean Data Assimilation Experiment (USGODAE) server was compared to the World Ocean Atlas 2009 (WOA09) in order to derive sensor errors (offset and drift) relative to the climatology. This procedure was repeated and float data were compared to discrete samples

Additional supporting information may be found in the online version of this article.

[1]Scripps Institution of Oceanography, University of California San Diego, La Jolla, California, USA.
[2]Monterey Bay Aquarium Research Institute, Moss Landing, California, USA.
[3]Maurice-Lamontagne Institute Mont-Joli, Quebec, Canada.
[4]School of Oceanography, University of Washington, Seattle, Washington, USA.
[5]CSIRO Marine and Atmospheric Research, Hobart, Tas, Australia.

Corresponding author: T. R. Martz, Scripps Institution of Oceanography, University of California San Diego, La Jolla, CA 92039, USA. (trmartz@ucsd.edu)

2169-9275/13/10.1002/jgrc.20399

for a limited number of instances, where those data were available concurrently. We report float specific correction coefficients for the entire array and contrast the two methods.

2. Methods

2.1. World Ocean Atlas 2009

[5] WOA09 is a monthly climatology on a 1° latitude-longitude grid from the surface to 5500 m at 33 standard depths for T, S, $[O_2]$ (μM), and oxygen percent saturation ($\%Sat = [O_2]/[O_{2Sat}] \times 100$, where $[O_{2Sat}]$ is the oxygen concentration at solubility equilibrium [*Garcia and Gordon*, 1992]). The units for $[O_2]$ were kept as μM since corresponding T and S data were not available to convert to μmol/kg. The $[O_2]$ and %Sat climatologies were created from over 800,000 and 700,000 QC'd discrete oxygen measurements, respectively, in the World Ocean Database 2009 (WOD09); all oxygen measurements were made by Winkler titration. The data went through further quality control by means of range checks as a function of depth and ocean region, statistical checks, and subjective flagging of data by the authors of the climatology. Relative to the mean climatological value, the standard error of data used to derive the climatology in the majority of the open ocean is 1–2 %Sat, except at depths where a strong oxycline exists [*Garcia et al*., 2010].

2.2. Profiling Float Data

[6] Profiling floats that measure oxygen are equipped with either a Sea-Bird SBE43 or an Aanderaa Optode. The SBE43 is a Clark-type electrode, where oxygen diffuses across a membrane and is converted to OH^- ion at the gold cathode and oxygen concentration is proportional to the induced current [*Edwards et al*., 2010]. The Optode is based on dynamic luminescence quenching, where the luminescence lifetime of a platinum porphyrine complex (the luminophore) is quenched in the presence of O_2. The luminophore is insulated by a gas permeable, optical isolation layer, and responds to the partial pressure of O_2 in air or solution [*Tengberg et al*., 2006]. The claimed accuracy of the factory calibration for the SBE43 is 2% and the Optode is 5% or 8 μM, whichever is greater; both sensors are calibrated between 0% and 120% saturation. For further details on both sensors, the reader is referred to *D'Asaro and McNeil* [2013].

[7] Profiling float data were downloaded from the USGODAE website in May 2012. A total of 473 floats were identified as "oxygen" floats, based solely on the presence of an oxygen variable in the float's NetCDF data file (see *Thierry et al*. [2011] for a complete list and definition of oxygen-related variables in profiling float NetCDF files). One hundred eighty-five of the 473 floats were rejected based on the procedure summarized in Figure 1 and 288 floats were compared to the WOA09. First, the two variables that contain dissolved oxygen concentration data, DOXY and MOLAR_DOXY, were inspected and 90 floats were rejected because the oxygen variables only contained NaNs, indicating no data was stored in the variable.

[8] Duplicate profiles, profiles with missing location data, and profiles with missing T, S, P, or $[O_2]$ data were removed. Data were rejected for $[O_2] > 550$ μM, approximately 10% larger than the highest $[O_2]$ in the WOA09.

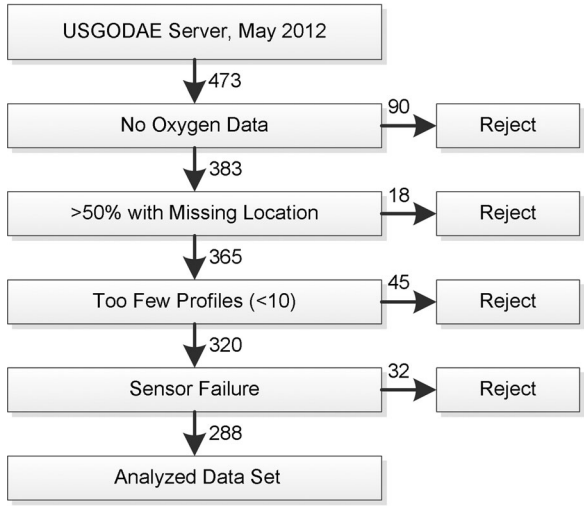

Figure 1. Flowchart of the selection process for floats deemed comparable to the WOA09. Numbers corresponding to the arrows represent the number of floats that were either rejected or accepted at each criterion.

The initial five profiles for floats equipped with the SBE43 were deleted prior to analysis, because these sensors can experience a rapid initial drift [*Martz et al*., 2008]. Floats with fewer than 10 profiles remaining after this process were rejected, leaving a minimum of 10 profiles to compare to the climatology. Furthermore, if over half of the profiles had missing location data, the float was rejected; this criterion was used as a proxy for floats in the vicinity of Antarctica where seasonal sea ice reduces the reliability of the climatology. This eliminated 63 floats.

[9] The oxygen data for the remaining 320 floats were visually inspected for spikes and qualitatively assessed for unreasonable profiles and apparent sensor failures. In most cases, sensor failures occurred stepwise or over a course of several profiles. The most common symptoms were negative $[O_2]$, entire profiles where $[O_2] = 0$ μM, or significant increase in $[O_2]$ with depth. In cases where the sensor failed middeployment, data until then were used if more than 10 "good" profiles remained. This rejected 32 floats (10 SBE43, 7 Optodes, and 15 unidentified), resulting in 288 floats for further analysis.

[10] Oxygen data under the variable DOXY were assumed to have been properly adjusted for salinity and pressure effects, as described by *Thierry et al*. [2011]. Salinity and pressure corrections were applied to the oxygen data under the MOLAR_DOXY variable only when the oxygen sensor was an Optode; it was assumed the data were listed in units of μM, salinity setting (S0) was 0 (default manufacturer setting), and the pressure coefficient was 3.2% 1000 dB^{-1} [*Uchida et al*., 2008]. %Sat was calculated following *Garcia and Gordon* [1992]. Quality controlled data distributed by the ARGO data centers (Delayed mode) for T, S, and P were used whenever available.

2.3. Comparison to the WOA09

[11] Climatological $[O_2]$ and %Sat values were first interpolated horizontally (by latitude and longitude) and temporally (by day of year) to the location and time of each float profile using a cubic spline method. If the profile was

taken within 1° latitude/longitude of a landmass, the nearest climatology location in space was used. Each resulting climatological profile was then interpolated vertically to the pressure or potential density measured by the float using cubic spline or linear methods, respectively. Linear interpolation was used for potential density surfaces because the spline method introduced significant noise (>10 μM) in weakly stratified regions of the water column, e.g., the surface mixed layer. Because vertical resolution of float measurements was equal to or higher than that of the climatology, no vertical averaging of the climatology was performed. For sensor drift calculations, oxygen concentrations from the climatology and float measurements were interpolated on 100 m intervals from 1500 to 2000 m.

2.4. Sensor Drift

[12] Sensor drift was determined as the average slope (least-squares regression) of the ΔO_2 versus time at depths between 1500 and 2000 m at 100 m intervals ($n = 6$), where $\Delta O_2 = [O_2]_{float} - [O_2]_{WOA}$. Sensor drift was calculated for floats with >1 year of data and ≥ 10 profiles deeper than 1500 m ($n = 170$). A trend in the deep ocean ΔO_2 was considered a proxy for sensor drift because the oxygen concentrations are very stable at this depth due to the lack of seasonal and annual signals [*Najjar and Keeling*, 1997]. In most cases, the residuals from the least-squares regression were slightly smaller when calculated on isopycnal surfaces than at constant depths because natural variability in the oxygen concentration due to vertical migration of isopycnal surfaces is accounted for. We therefore report sensor drift based on isopycnal surfaces (Table S1 in the supporting information). Four outliers (WMOID 5900345, 5902305, 5902308, and 5903260) were removed because the ΔO_2 time series changed stepwise when entering another water mass (most likely a mesoscale feature not captured in the climatology), unevenly distributed deep O_2 data biased the slope, or it was clear that the change in deep ΔO_2 was not due to sensor drift (see section 4 for details). This resulted in 166 floats analyzed for drift.

[13] Of the 166 floats, 74 exhibited sensor drift at the 95% CI based on a *t*-test (*t*-test, $p < 0.05$, df = 5) indicating a detectable drift relative to the climatology (labeled in Table S1). Sensor drift corrections were only applied to these floats prior to further analysis. This filtering criterion was applied to avoid overcorrecting the float data due to errors arising from uncertainties in the climatology (see section 4).

2.5. Oxygen Correction Coefficients

[14] Float specific oxygen dependent correction terms were determined by performing a model II linear regression [*York*, 1966] on $[O_2]_{float}$ versus $[O_2]_{WOA}$ and $\%Sat_{float}$ versus $\%Sat_{WOA}$ (Figure 2).

$$[O_2]_{WOA} = C_{0,[O2]} + C_{1,[O2]} \times [O_2]_{float} \quad (1)$$

$$\%Sat_{WOA} = C_{0,\%Sat} + C_{1,\%Sat} \times \%Sat_{float} \quad (2)$$

[15] The model II linear regression was used because there are errors associated with both float and WOA data. The $|\Delta O_2|$ increases in magnitude in strong vertical oxygen gradients due to a combination of dynamic sensor errors (e.g., response time and thermal lag), smoothing of real gradients in the WOA by averaging over multiple profiles, and natural vertical migration of the isopycnal surfaces by processes such as internal waves. Oxygen measurements taken in vertical gradients where $|\partial[O_2]/\partial z| > 0.2$ μM m^{-1} were omitted from the regression in order to minimize these errors. The corrected float oxygen, $[O_2]_{float}$ and $\%Sat_{float}$, was calculated by

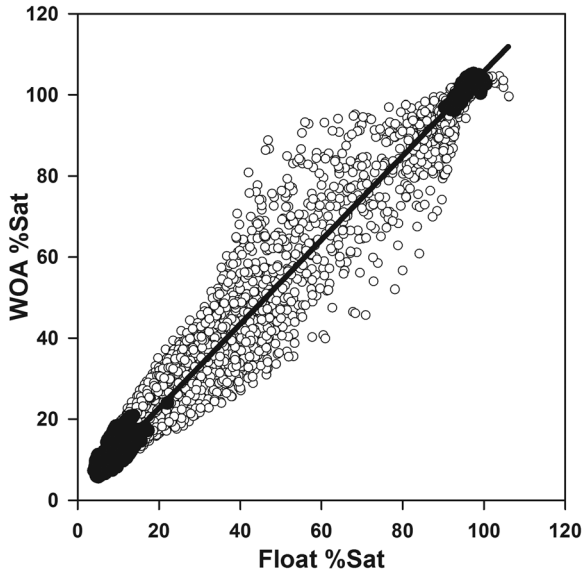

Figure 2. Plot used to calculate C_1 and C_0 for a float (WMO ID: 4900523). The data used and omitted ($|\partial O_2/\partial z| > 0.2$ μM m^{-1}) are represented by black circles and open circles, respectively. The solid line is the model II linear regression.

$$[O_2]_{float}' = C_{0,[O2]} + C_{1,[O2]} \times [O_2]_{float} \quad (3)$$

$$\%Sat_{float}' = C_{0,\%Sat} + C_{1,\%Sat} \times \%Sat_{float} \quad (4)$$

where C_0 (offset) and C_1 (gain) are the coefficients from the model II regression. The standard error (SE) of the coefficients, and the root-mean-squared error (RMSE) of the fit are reported.

[16] Note that the proposed correction terms do not account for dynamic errors due to slow sensor response. At the present time, dynamic errors cannot be addressed for the global float oxygen data set because the errors are specific to sensor make and model, and this information is not necessarily documented in the metadata. Fortunately, the error is small in regions of low vertical oxygen gradient (see section 4), and thus restriction of data to these regions minimizes this bias.

2.6. Discrete Samples Near Float Profiles

[17] We (Riser, Johnson, and Gilbert) have deployed several floats near oceanographic time series stations (HOT, BATS, and Line *P*) and a repeat hydrography transect (CLIVAR section I06S), providing a unique opportunity to compare float sensor data to discrete samples taken near the time and location of a float profile (Table 1, $n = 14$, referred to as FloatVIZ floats hereafter). FloatVIZ

Table 1. FloatVIZ Correction Terms

Float	Days Apart	Distance (km)	$C_{0,\text{Bottle}}$ [%Sat]	$C_{0,\text{WOA}}$ [%Sat]	$C_{1,\text{Bottle}}$	$C_{1,\text{WOA}}$	RMSE Bottle [μM]	RMSE WOA [μM]	$O_2' - O_{2,\text{Bottle}}$ (Surface) [μM (%Sat)][a]	$O_2' - O_{2,\text{WOA}}$, (Surface) [μM (%Sat)][a]	$O_2' - O_{2,\text{Bottle}}$ (Min. O_2) [μM (%Sat)]	$O_2' - O_{2,\text{Bottle}}$ (Min. O_2) [μM (%Sat)]
5143[b,c,d]	3	20	−1.591	1.300	1.122	1.099	1.46	3.79	28.8 (9.7)	31.1 (10.4)	−3.0 (−0.9)	6.2 (1.9)
5145[b,d,e]	2	14	0.526	1.040	1.066	1.092	2.74	7.04	14.5 (6.8)	20.7 (9.6)	2.8 (0.9)	4.8 (1.5)
5146[b,d,f]	3	17	6.730	10.484	1.009	0.950	2.40	6.91	25.3 (7.6)	19.5 (5.8)	24.1 (7.1)	27.6 (8.2)
6391[b,d,g]	4	17	10.211	11.846	0.971	0.951	2.33	5.85	16.3 (7.5)	15.8 (7.3)	24.8 (8.9)	26.9 (9.6)
6401[b,d,e]	3	102	1.368	2.175	1.041	1.012	6.15	7.80	11.3 (5.4)	7.0 (3.3)	5.0 (1.6)	7.0 (2.2)
6403[b,d,e]	2	10	0.111	0.734	1.074	1.073	2.94	6.77	15.1 (7.1)	16.4 (7.7)	1.9 (0.6)	3.9 (1.2)
6891[b,d,e]	3	8	1.583	0.881	1.040	1.038	4.05	8.09	11.8 (5.6)	9.8 (4.6)	5.9 (1.9)	3.6 (1.2)
6976[b,d,e]	2	10	8.343	14.407	1.044	0.950	2.90	6.91	28.2 (12.3)	22.8 (9.9)	28.6 (10.3)	33.7 (12.2)
4900093[c,h,i]	12	14	0.651	1.877	1.066	1.031	2.67	6.42	14.9 (7.0)	10.4 (4.9)	3.1 (1.0)	6.5 (2.0)
4900235[c,h,i]	5	207	0.753	1.601	1.065	1.037	5.30	4.80	20.8 (6.9)	15.4 (5.1)	3.4 (1.0)	5.9 (1.7)
4901153[c,h,i]	2	63	−1.587	1.554	0.913	0.845	4.25	3.88	−34.4 (−11.8)	−48.4 (−16.6)	−6.6 (−2.0)	2.5 (0.8)
5900952[c,h,i]	12	19	−0.311	0.818	1.039	1.055	9.06	10.89	7.0 (3.3)	12.7 (6.1)	−0.1 (0.0)	3.9 (1.2)
5901069[d,e,h]	3	29	−0.348	0.840	1.105	1.050	4.27	9.24	20.8 (9.8)	12.0 (5.6)	1.3 (0.4)	3.9 (1.2)
5901336[d,e,h]	3	166	−0.818	−1.182	1.091	1.077	3.00	7.03	16.7 (6.2)	13.2 (6.2)	−1.0 (−0.3)	−2.4 (−0.7)
Average	5	50	1.83	3.46	1.05	1.02	3.82	6.81	14.1 (6.1)	11.3 (5.0)	6.44 (2.17)	9.58 (3.16)
SD.	4	64	3.76	4.89	0.05	0.07	1.96	1.92	15.4 (5.6)	18.3 (6.6)	11.01 (3.76)	11.1 (3.9)

[a] O_2' refers to corrected O_2 ([O_2] and %Sat) using equations (3) and (4).
[b] Float data downloaded from http://www.mbari.org/chemsensor/floatviz.htm.
[c] Discrete sample collected on line P (Including Ocean Station Papa).
[d] Float equipped with Optode.
[e] Discrete sample collected at HOT.
[f] Discrete sample collected on the CLIVAR repeat section I06S.
[g] Discrete sample collected at BATS.
[h] Float data downloaded from USGODAE website.
[i] Float equipped with SBE43.

data were downloaded from http://www.mbari.org/chemsensor/floatviz.htm and the USGODAE website. Corresponding discrete samples were downloaded from the time series' websites or provided directly from PIs for data not yet publically available.

[18] O_2 from the hydrographic casts was interpolated vertically for comparison to the float data on isobaric (dbar), isothermal (θ), and isopycnal (σ) surfaces corresponding to float measurement points. C_0 and C_1 for [O_2] and %Sat were calculated on the three different vertical grids, for a total of six different combinations. Finally, the corrected oxygen data based on the discrete samples and WOA09 were compared.

2.7. Recalibration of Optode Sensors

[19] Seven float Optodes (Aanderaa model 3830) were calibrated at CSIRO, achieving an accuracy of <1 μM throughout the oceanic range of temperature and O_2. The sensor response (phase shift) was recorded at eight different values of [O_2] between 0 %Sat and 130 %Sat, and repeated at five different temperatures between 1°C and 30°C ($n = 40$). Response of each sensor was calibrated to oxygen concentration determined by triplicate Winkler titration. Data were fit to the Stern-Volmer equation using a nonlinear multivariate regression [*Uchida et al.*, 2008]. The average root-mean-squared error (RMSE) of the fit for the seven Optodes was 0.60 ± 0.05 μM (1σ).

3. Results

3.1. Sensor Drift

[20] Sensor drift was categorized by sensor type, i.e., SBE43 or Optode (Figure 3). The average sensor drift for all floats was 0.2 ± 2.8 μM yr^{-1} (1σ, $n = 166$). The average Optode and SBE43 drift was 0.9 ± 2.7 μM yr^{-1} (1σ, $n = 102$) and -1.0 ± 2.7 μM yr^{-1} (1σ, $n = 62$), respectively. Sensor type was unidentified for two of the 166 sensors, resulting in a total of 164 floats for this comparison. A higher percentage of floats equipped with SBE43 (53%) had a detectable drift relative to the climatology (i.e., sensor drift significantly different than 0 at the 95% CI) compared to Optodes (37%).

3.2. Float Oxygen Correction

[21] When comparing float data to discrete data, corrections based on %Sat on isobaric surfaces yielded the lowest standard error for C_1 (SE_{C1}) (Table 2); although the improvement was not statistically significant when switching from [O_2] to %Sat ($p > 0.15$), or changing the vertical grid ($p > 0.1$). However, corrections based on %Sat are

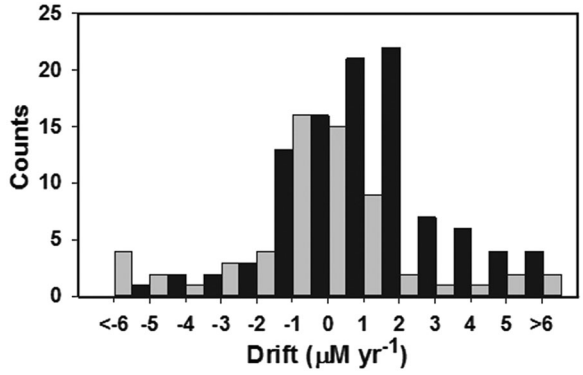

Figure 3. Histogram showing the frequency of sensor drift by sensor type: Optode (black, $n = 105$) and SBE43 (gray, $n = 63$).

Table 2. Mean Standard Error for $C_1 \pm$ SD for FloatVIZ Floats[a]

	$[O_2]$	% Sat
P	0.017 ± 0.015	0.011 ± 0.005
σ	0.018 ± 0.015	0.015 ± 0.011
θ	0.020 ± 0.014	0.017 ± 0.012

[a]Results from linear regression of FloatVIZ versus discrete samples, interpolated onto isobaric (P), isothermal (θ), or isopycnal (σ) surfaces using $[O_2]$ and %Sat ($n = 14$). The SD is calculated from the 14 SE_{C1} from FloatVIZ floats.

probably preferable because $[O_2]$ responds rapidly to changes in solubility that are driven by temperature, and using %Sat would largely correct for these changes. Since the climatology is gridded on isobaric surfaces, unless otherwise noted, correction coefficients hereafter were calculated using %Sat on isobaric surfaces and referred to simply as C_0 and C_1.

[22] The correction results based on both discrete samples and the WOA09 for the FloatVIZ floats are summarized in Table 1. On average, RMSE was lower for bottle corrections compared to WOA corrections (3.8 versus 6.8 μM); although, due to the high number of samples, SE for floats versus WOA (see Table S1) is lower than SE reported in Table 2 for float versus discrete samples. On average, the two methods agreed well; the difference of the applied correction (WOA – discrete) at the surface was -2.8 ± 5.5 μM, or -1.06 ± 2.2 %Sat (1σ).

[23] Correction coefficients of the 288 floats from the USGODAE server are shown in Figure 4 and reported in Table S1. The correction coefficients for six floats were rejected (noted in Table S1) after visual inspection indicated abrupt changes in temperature, salinity, and O_2 in the floats with no corresponding changes in $O_{2,WOA}$. This was

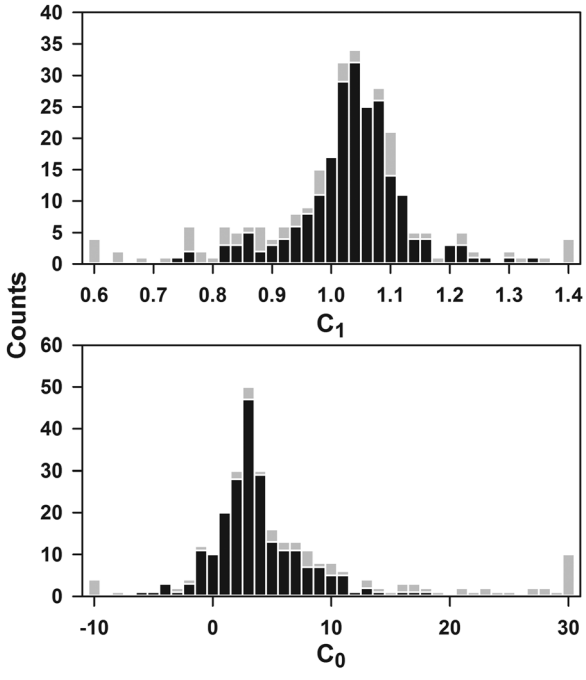

Figure 4. Stacked bar plot of the slope (C_1) and intercept (C_0) ($n = 282$). Floats where $SE_{C1} < 0.006$ ($n = 217$) and $SE_{C1} > 0.006$ are shown in black and gray, respectively.

most likely due to water masses not accurately captured by the climatology (e.g., interannual variability of frontal zones); these floats are not included in further discussions. The average Δ%Sat at the surface, where $\Delta\%Sat = \%Sat_{float} - \%Sat_{WOA}$, was -6.11 ± 8.8 (1σ) %Sat precorrection and -0.37 ± 2.3 %Sat post correction. The mean ($\pm 1\sigma$) C_0, C_1, and RMSE [μM (%Sat)] calculated from equation (4) for all floats was 5.47 ± 9.4, 1.01 ± 0.14, and 8.9 (2.99%) $\pm$ 3.0 (1.1%), respectively.

4. Discussion

4.1. Sensor Drift

[24] Of the 166 floats analyzed for sensor drift, less than half had a detectable drift relative to the climatology ($n = 74$). This result shows that the majority of oxygen profiling floats are stable for years. The climatology is constructed using historical data spanning many decades, but the sampling is sparse in both time and space. This complicates using the climatology to correct a data set that is relatively short term in length. A climatology-based correction is therefore prone to errors in areas where deep oxygen is subject to short-term variability due to deep ventilation such as frontal zones and the subpolar North Atlantic, potentially creating a bias in the calculated drift. For example, *Stendardo and Gruber* [2012] show interannual variability of O_2 as large as 15 μM in the North Atlantic Intermediate Water ($\sim$800–900 m), and the majority of the floats with detectable "drift" were in fact located in the North Atlantic.

[25] For most of the floats with detectable drift, including all those equipped with an Optode sensor, a positive drift was just as likely as a negative drift, relative to the climatology. Experience with drift of the SBE43 [*Gruber et al*., 2010] and observed shifts in Optode calibrations [*Bushinsky and Emerson*, 2013; *D'Asaro and McNeil*, 2013] all indicate that these sensors primarily drift toward lower reported oxygen concentration. This suggests that short-term variability in oxygen distributions relative to the climatology introduces significant uncertainty in the calculated sensor drift, in both a positive and negative direction.

[26] Only for the SBE43 is there seen to be a second mode in the frequency histogram of sensor drift (Figure 3), suggesting that some of these sensors do experience significant drift, a result consistent with previous observations [*Gruber et al*., 2010; *Martz et al*., 2008]. Studies have shown that Optodes on profiling floats produce highly stable data for years [*Körtzinger et al*., 2005; *Tengberg et al*., 2006], which agrees with the indication that changes of the Optode sensor, relative to climatology are due to changes in ocean oxygen distributions or errors in the climatology. However, since the number of floats in the second mode (and possibly a third in the high extreme) is small, it is difficult to say with confidence if this phenomenon is real. Further independent data are necessary to verify these results.

[27] Comparing float oxygen data to a regional climatology based on recent historical data, an approach adopted by the ARGO community to QC salinity data [*Owens and Wong*, 2009], would better address the question of sensor drift. Unfortunately, currently, there is no global oxygen

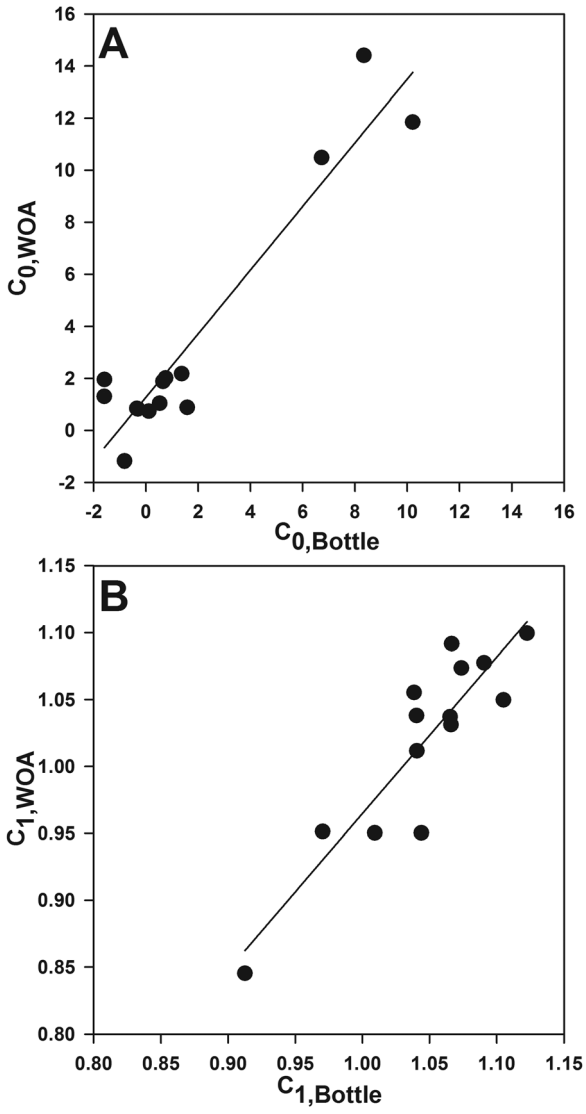

Figure 5. Scatter plot of (a) $C_{0,\%Sat}$ and (b) $C_{1,\%Sat}$ for the 14 FloatVIZ floats from bottle samples and the WOA. Linear regressions, shown as solid lines, yielded $R_{C1} = 0.89$, $R_{C0} = 0.94$.

data set that is dense enough to apply this method for float oxygen. However, it is encouraging that the majority of floats showed no drift in this study, suggesting that an array of properly calibrated floats is capable of producing a reliable oxygen data set for biogeochemical studies.

4.2. Method Assessment

[28] The comparison of WOA versus discrete sample correction coefficients for the 14 FloatVIZ floats shows a strong correlation between the two methods (Figure 5, $R_{C1} = 0.89$, $R_{C0} = 0.94$), suggesting that the two methods are correcting for similar sources of error. The average difference between the two corrections (1.1 ± 2.2 %Sat at the surface, Table 1) suggests that either approach is capable of improving the first-order errors often observed in factory sensor calibrations. For the bottle-based correction, the implicit assumption is made that a single cast is sufficient to provide a reliable correction throughout the life of the float. Local gradients and timing mismatch between a single hydrographic profile and a float profile, or rapid initial sensor drift in the case of SBE43 can lead to errors in this approach. As seen in Table 1, most discrete samples are taken days, and tens of kilometers apart from the profiling float; in other cases the spatial and temporal discrepancies may be even larger. Any natural processes that alter oxygen concentrations during that interval in space and time (e.g., temperature changes in the mixed layer) would lead to errors in the correction terms derived from a single hydrographic profile. On the other hand, the climatology-based approach is data limited over large regions of the ocean, leading to increased uncertainty in the correction coefficients (Figure 6). Nonetheless, the agreement between the two methods implies that either approach is capable of correcting the float oxygen data to several %Sat at the surface.

[29] The benefit of a WOA-based correction is that it provides a postdeployment QC protocol for all floats. The vast majority of oxygen floats are not deployed with a corresponding hydrographic cast. As oxygen sensors become a mainstay on profiling floats, increasing numbers will be deployed from ships without the capability to perform hydrographic casts. For example, many of the profiling floats in the Argo program are deployed from Ships of

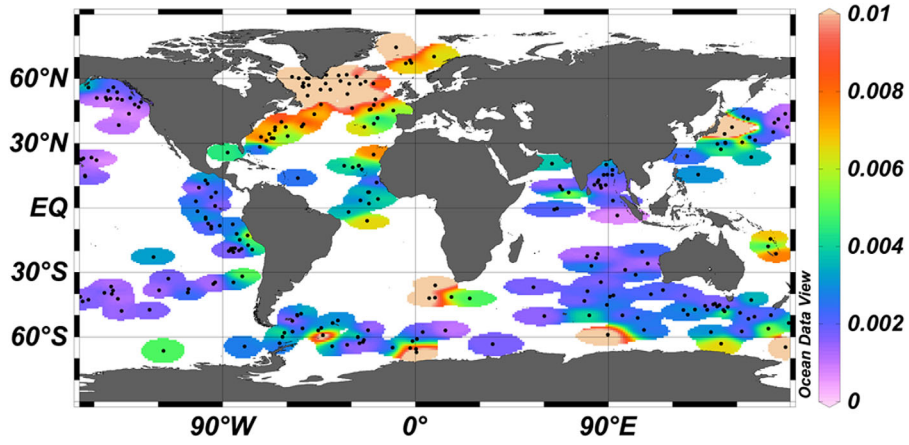

Figure 6. Distribution of SE_{C1} from equation (2). Location of floats was determined by mean latitude and longitude. Majority of high SE_{C1} values are observed in the North Atlantic.

Opportunity to achieve the target global coverage of the array. If profiling floats with oxygen sensors are to reach coverage similar to the existing Argo array, QC methods applicable to all floats will be a critical requirement.

[30] The global distribution of the standard error of C_1 (SE_{C1}) suggests that this method is more robust in certain regions than in others (Figure 6). A low SE_{C1} results from a properly functioning oxygen sensor, combined with an accurate representation of O_2 in the climatology through the entire O_2 range experienced by the float. A high SE_{C1} suggests an error in either sensor or climatology (or both). It is clear that the majority of floats with a high SE_{C1} are located in the North Atlantic, which strongly suggests that the method is less robust in this basin. A SE_{C1} threshold of 0.006 (the highest observed for the FloatViz floats versus WOA) was chosen to select floats with agreement to the climatology similar to the 14 FloatViz floats. Two hundred twenty profiling floats remained after this final filtering criterion was applied, eliminating most floats at latitudes north of 30°N in the Atlantic (Table S1). The C_0 and C_1 ($\pm 1\sigma$) of the remaining 220 floats are 3.22 ± 3.7 and 1.02 ± 0.09, respectively, and the average surface Δ%Sat improved from -5.19 ± 7.9 %Sat to -0.20 ± 2.3 %Sat. Thus on average, float oxygen data were corrected by about 5 %Sat at solubility equilibrium (i.e., $3.22 + 1.02 \times 100 - 100 = 5.2$). The relatively large uncertainty range of ± 7.9 %Sat indicates that many floats are likely to disagree with the WOA by more than 10 %Sat at equilibrium, due to both calibration error and errors in the WOA.

[31] The correction coefficients for floats rejected in this final criterion are not necessarily unreliable. For example, regression analysis through a narrow range of O_2 can lead to high SE_{C1}, but provide sufficient C_1 and C_0 for that O_2 range. However, applying coefficients for such floats outside of the observed O_2 range is suspect, and should be avoided.

[32] The correction coefficients for the 220 floats were separated by sensor type (Table 3). C_0 for both sensors and C_1 for SBE43 were significantly different from 0 and 1, respectively at the 99.99% confidence level ($p < 0.0001$), whereas C_1 for the Optode was not statistically different from unity ($p = 0.30$). A *t*-test analysis showed that both C_0 and C_1 between the two sensors were significantly different ($p < 0.01$), suggesting a possible difference between the quality of factory calibration. On average, it seems that Optodes tend to be biased low by a constant %Sat, whereas the SBE43 has an error in gain. However, the large standard deviation of the coefficients for both sensors indicates that the quality of calibration varies significantly from sensor to sensor.

4.3. Corrections in Low Oxygen Regimes

[33] Recent studies suggest that the World Ocean Atlas overestimates O_2 in most suboxic/anoxic regions [*Fuenzalida et al.*, 2009; *Bianchi et al.*, 2012], therefore O_2' in low oxygen regimes may be overestimated. This error is clearly demonstrated by a float equipped with both an Optode and an ISUS nitrate sensor that was deployed in the eastern tropical Pacific by Riser and Johnson (Figure 7) [*Johnson et al.*, 2013]. The $[O_2]_{float}$ is <1 μM for several hundred meters in the core of the oxygen minimum zone (OMZ), whereas $[O_2]_{WOA}$ ranges from 5 to 32 μM. The

Table 3. Correction Coefficients Divided by Sensor Type for Floats Where $SE_{C1} < 0.006$

	Optode ($n = 130$)	SBE43 ($n = 87$)
C_0 [%Sat] ± SD	4.33 ± 3.5	1.96 ± 3.2
C_1 ± SD	1.007 ± 0.098	1.044 ± 0.067

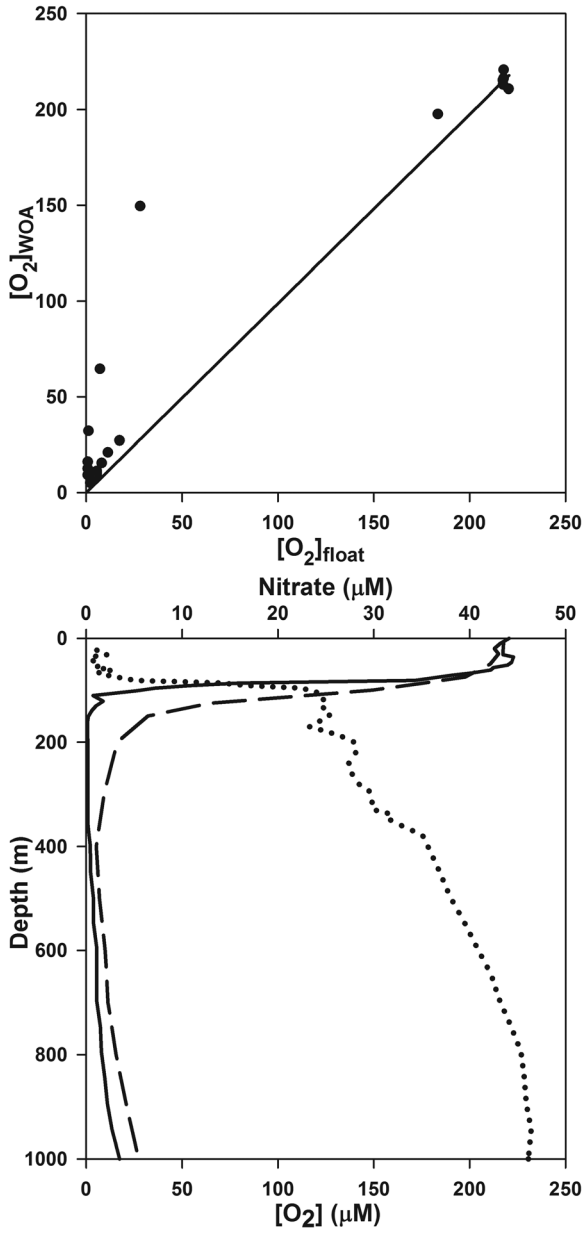

Figure 7. (top) Comparison of $[O_2]_{float}$ to $[O_2]_{WOA}$ demonstrates the mismatch at low O_2 (FloatVIZ ID: 7558). Climatology oxygen values are positive in the oxygen minimum, while the float is nearly zero (<1 μM). The line shown is a linear regression using only the surface value (forcing the *y* intercept through zero). (bottom) profiles from $[O_2]_{float}$ (solid line), $[O_2]_{WOA}$ (dashed line), and $[NO_3^-]_{float}$ (dotted line). Reversal of nitrate is indicative of nitrate reduction, and float oxygen values are <1 μM in this region.

inversion of the nitrate profile in the same depth range provides strong evidence of water column denitrification, which only occurs under anoxic conditions, confirming that $[O_2]_{float}$ is more accurate than $[O_2]_{WOA}$ for this particular float near zero $[O_2]$.

[34] A similar trend was observed for the global float array. $[O_2]_{float}$ in known permanent anoxic OMZs (northern Indian Ocean and eastern tropical Pacific) ranged between 0 μM and 5 μM, whereas the corresponding $[O_2]_{WOA}$ were 6–12 μM. This is in good agreement with *Bianchi et al*. [2012], who show an average bias in the WOA of +6 μM in hypoxic regions. These results suggest that oxygen sensor calibration is robust at low O_2 [*D'Asaro and McNeil*, 2013], and a positive offset correction is not appropriate for floats in OMZs. A correction based on equation (2) will bias the offset high due to this error in the climatology. For such floats, only adjusting the gain while forcing the offset to 0 should minimize this error.

[35] One straightforward approach to calculate the gain is to compare the surface $\%Sat_{float}$ to the surface $\%Sat_{WOA}$ using >1 year of data, i.e., $C_1 = \text{mean}\ (\%Sat_{WOA}/\%Sat_{float})$ at the surface (Table S1). It is counterintuitive to restrict the float O_2 data to the most dynamic region of the water column to obtain correction coefficients. However, due to rapid gas exchange and a constant atmospheric oxygen concentration, %Sat remains very close to solubility equilibrium at the surface over an annual cycle [*Najjar and Keeling*, 1997]. Therefore, a robust estimate of the gain can be obtained from $\geq$1 year of surface data. This method is appealing due to its simplicity; however, it has one large drawback: float oxygen data corrected using this method cannot provide an independent estimate of net community production (NCP). Most of the ocean is a few %Sat above solubility equilibrium when averaged annually, due to biological activity and bubble injection [*Hamme and Emerson*, 2006]. If float oxygen data are corrected to the average annual surface %Sat of the WOA09, then subsequent calculations of NCP will always reflect biological activity that is necessary to maintain the level of supersaturation in the climatology. Therefore, studies of biological production in the euphotic zone would be biased by this simple correction. In order to obtain independent estimates of NCP using profiling float oxygen data, a calibration protocol that enables the sensors to constrain oxygen concentrations more accurately than the climatology must be established.

4.4. Sources of Oxygen Sensor Error

[36] Sources of error in float oxygen can be categorized as either calibration errors or dynamic errors (Table 4). The method described here corrects for the calibration errors and sensor drift (a dynamic error); yet, it is important to keep in mind that other dynamic errors remain uncorrected. At minimum, correction of dynamic errors beyond sensor drift requires knowledge of sensor manufacturer, model, and calibration coefficients. These values are not sufficiently tabulated in the global float oxygen metadata, making it impractical for any single research group to analyze the data set as a whole for dynamic errors. However, a brief discussion on dynamic errors of the Aanderaa Optode is warranted, as this has been the dominant sensor deployed in the global float array for many years. For a detailed review on the SBE43, the reader is referred to *Edwards et al*. [2010].

Table 4. Sources of Errors for Profiling Float Oxygen

Error Type	Correction
Calibration Errors	
$[O_2]$ and T coefficient(s)	Apply linear correction using C_0, C_1 [this work]
Pressure coefficient(s)	3.2%/1000 dBar [*Uchida et al*., 2008]
Dynamic Errors	
Delayed T response	Use sensors equipped with fast response thermistor
Response time	Use oxygen gradient with τ fit [this work]
Drift	Linear regression on ΔO_2 [this work]

[37] Delayed temperature errors arise when there is a thermal disequilibrium between the sample water in contact with the oxygen sensing element and the thermistor. The resulting oxygen measurements are affected by temperature through (1) the temperature dependency of the sensor itself and (2) the $[O_{2Sat}]$ temperature dependence used to convert the raw sensor output (phase shift) to oxygen concentration [*Garcia and Gordon*, 1992]. The thermistor is embedded deep inside of the sensor for the Model 3830, the most common Optode model deployed on profiling floats, leading to a greater potential for thermal disequilibrium. Discrepancies between the temperature reading from the CTD and these Optodes can frequently be as large as 1.5°C. The oxygen error due to this temperature discrepancy is sensor specific and can only be quantified if the temperature response of the sensor is well characterized. Two randomly selected Optodes generated errors on the order of 15 μM for a 1.5°C shift in input temperature. An accurate estimate of the probable range of this error within the float array would require access to a distribution of calibration coefficients from many sensors, data which were not publicly available at the time of this work. Preliminary results from Optodes with a faster thermistor response (Model 4330F) suggest improved performance [*Riser*, 2012]. However, this sensor model was only recently introduced into the float array and its performance was not assessed in this study.

[38] The Optode response time to oxygen ($\tau \sim$23 s at 25°C) [*Uchida et al*., 2008] can lead to significant errors when a float ascends through a strong oxygen gradient. The actual oxygen concentration can be estimated ($[O_2]_{model}$) from the reported concentration ($[O_2]_{float}$) based on the oxygen gradient and τ as

$$[O_2]_{model} = [O_2]_{float} - \tau \frac{\partial [O_2]}{\partial t} \left(1 - e^{\left(-\frac{t}{\tau}\right)}\right) \quad (5)$$

where $\partial[O_2]/\partial t$ is the oxygen gradient with respect to time, assuming a float ascent rate of 10 cm s^{-1}. This simple model was created based on equations used to model thermal lag of profiling CTDs [*Johnson et al*., 2007]. Previous work suggests that τ is temperature dependent (longer at lower temperatures), and may be sensor specific [*Uchida et al*., 2008]. The modeled oxygen error resulting from different τ using an actual profile is shown in Figure 8. When a constant τ of 30 s throughout the profile is assumed, oxygen errors as large as 15 μM were calculated during the strongest oxygen gradient ($\sim$5 μM m^{-1}). It is noteworthy

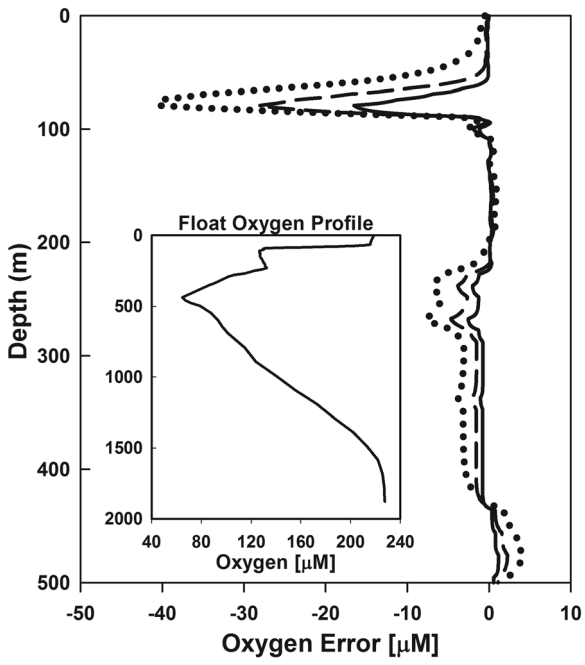

Figure 8. The depth profile of the modeled oxygen error ($[O_2]_{float}$–$[O_2]_{model}$) for float 1900650 on 4 September 2007 between 0 and 500 m, assuming a τ of 30, 60, and 120 s (solid, dashed, and dotted lines, respectively). Inset shows the full oxygen profile.

that such a large oxygen gradient is rare, and a more commonly observed gradient of 1 μM m^{-1} results in a $\sim$6 μM error. However, due to uncertainties associated with τ, this correction was not applied to the float oxygen data. Since data were selected from regions where $|\partial[O_2]/\partial z| < 0.2$ μM m^{-1}, the errors due to slow sensor response should be minimal. In order to accurately correct this error, further investigation on sensor response over a range of temperature and pressure is required.

4.5. Laboratory Predeployment Calibration of Optodes

[39] A float data set, corrected to the WOA09, will reflect any errors inherent to the climatology; this may not be satisfactory for some biogeochemical studies. For example, independent estimates of NCP require the accuracy of the oxygen measurements to be <1 %Sat near the surface [*Emerson et al*., 2008]. Currently, the uncertainties inherent to the climatology are slightly larger than this requirement (1–2 %Sat for large parts of the surface ocean) due to sparse sampling in both time and space. A more direct and straightforward approach would be to properly calibrate the sensors prior to deployment. The Optode can achieve an accuracy of $\sim$1 μM between 0°C and 30°C when individual sensors are calibrated against discrete samples analyzed by Winkler titration [*Bittig et al*., 2012; *Bushinsky and Emerson*, 2013; *D'Asaro and McNeil*, 2013]. This is a significant improvement over the current factory calibration for Optodes, which claims an accuracy of "5% or 8 μM, whichever is larger." Discrepancies larger than the claimed accuracy have been reported [*Kobayashi et al*., 2006] and were also observed in this study as described above. To our knowledge, most, if not all oxygen data archived at USGODAE uses factory derived calibration coefficients. Thus, an establishment of a proper sensor calibration protocol is a critical step to meet the stringent requirements desired by the community.

[40] In 2011, Tilbrook and Neill deployed seven floats in the Southern Ocean equipped with Optodes that were recalibrated in-house. Correction coefficients from the WOA were calculated using both the factory calibrations and the laboratory recalibrations (Table 5). The C_1 obtained using laboratory recalibrated sensors was significantly closer to unity (1.02 ± 0.02 and 1.08 ± 0.02 for recalibration and factory calibration, respectively), reflecting the improved calibration protocol. On average, the laboratory calibrations agreed with the WOA by $\sim$5 %Sat at the surface, compared to $\sim$17 %Sat for the factory calibrations.

[41] Even after laboratory recalibration, all seven Optodes recorded oxygen values that were low relative to the WOA ($C_0 = 3$, Table 5), suggesting either a bias in the climatology in this region, or an unidentified mechanism occurring between calibration and deployment that systematically decreases the sensor measurement. A decrease in sensor response (i.e., a drift toward lower oxygen concentration) for Optodes was also observed in recent studies and attributed to decreased oxygen sensitivity of the sensor [*Bushinsky and Emerson*, 2013; *D'Asaro and McNeil*, 2013]. However, based on previous observations [*Körtzinger et al*., 2005; *Tengberg et al*., 2006] and results from this study, data from Optodes deployed on profiling floats are stable for years. One hypothesized mechanism that explains these two seemingly contradictory observations is migration/diffusion of the luminophore in the oxygen sensing foil over time, leading to lower oxygen values. This effect would be temperature dependent and minimal at low temperatures, providing an explanation for the observation that Optodes on profiling floats are stable for years (floats spend the majority of the time in the cold deep ocean). Further mechanistic studies of this phenomenon are necessary to establish a stringent calibration and storage protocol for oxygen sensors. However, it is encouraging that recalibrated sensors exhibited significantly better agreement with the WOA. We therefore recommend that researchers contributing to the global oxygen float array recalibrate oxygen sensors prior to deployment.

5. Conclusions

[42] Float specific oxygen sensor correction terms for 288 profiling floats are reported based on a comparison to

Table 5. Correction Coefficients for Laboratory Recalibrated Optodes

Float	$C_{0,\ Factory}$	$C_{0,\ Lab}$	$C_{1,\ Factory}$	$C_{1,\ Lab}$
1901152	7.744	2.761	1.059	0.991
1901153	6.385	2.278	1.085	1.030
1901154	5.874	2.824	1.099	1.022
1901155	6.056	1.191	1.111	1.051
1901157	6.780	4.382	1.075	1.007
1901158	6.798	2.480	1.057	1.004
1901159	7.437	3.678	1.078	1.014
Avg $\pm$ SD	6.72 ± 0.69	3.00 ± 1.14	1.08 ± 0.02	1.02 ± 0.02

the World Ocean Atlas. The correction approach was validated for a small subset of the global array where additional information (bottle samples or sensor recalibration) was available. The corrections were shown to improve the sensor data reported in the USGODAE database. The results suggest that the corrected float oxygen values constrain oxygen concentrations to several %Sat at the surface. Oxygen data from floats deployed at high latitude in the North Atlantic and parts of the Southern Ocean deviated from a simple linear relationship with the climatology, suggesting this method is not robust in these areas due to complex hydrography and/or sparse coverage in the WOA. Correcting float data in areas with low O_2 by only adjusting the gain may be more appropriate.

[43] Further limitations of the correction based on gain only should be noted. For floats deployed in areas where there is a weak oxygen gradient throughout the water column (e.g., North Atlantic or Southern Ocean), applying a gain-only correction can introduce errors of up to 5% in the midwater column relative to the climatology. This could be due to uncharacterized dynamic sensor errors, redistribution of oxygen in the midwater column, nonlinear response of the sensor to [O_2], or improperly characterized temperature coefficients. Overall, a gain-only (C_1) correction, applied to floats in OMZs, coupled with an offset + gain correction (C_0 and C_1) for all other floats would likely produce the most accurate float oxygen data set, given the present limitations of the WOA. Accordingly, the coefficients for both corrections are reported in Table S1.

[44] In order for float data to be used to improve upon the climatology, the accuracy of the calibration protocol must be better than the errors in the climatology, i.e., 1–2 %Sat for most of the world's oceans. Ideally, float oxygen data from sensors that have undergone a proper calibration protocol would be verified using a climatology based on recent historical data; an approach adopted for float salinity data QC. However, due to the uncertainties associated with the WOA09 as discussed above, this approach seems currently untenable unless there is a significant increase in the number of independent oxygen measurements. One promising alternative is to validate oxygen measurements in situ using atmospheric oxygen measurements [*Bushinsky and Emerson*, 2013], a methodology that has yet to be tested on profiling floats. The calibration process, however, is not necessarily trivial, is labor and time intensive, and may cost as much as the sensor itself; a fact often underappreciated by the scientific community. Consequently, the most practical solution would appear to be agreement of the community to send Optode sensors to a certified facility(s) capable of high accuracy calibration, until it can be demonstrated that factory calibrations are of equal quality.

[45] **Acknowledgments.** This work was supported by NOPP award N00014-10-1–0206. We would like to thank Steve Emerson and Rod Johnson for providing discrete sample data that were not publically available.

References

Bianchi, D., J. P. Dunne, J. L. Sarmiento, and E. D. Galbraith (2012), Data-based estimates of suboxia, denitrification, and N_2O production in the ocean and their sensitivities to dissolved O_2, *Global Biogeochem. Cycles*, *26*, GB2009, doi:10.1029/2011GB004209.

Bittig, H. C., B. Fiedler, T. Steinhoff, and A. Körtzinger (2012), A novel electrochemical calibration setup for oxygen sensors and its use for the stability assessment of Aanderaa Optodes, *Limnol. Oceanogr.Methods*, *10*, 921–933, doi:10.4319/lom.2012.10.921.

Bohme, L., and U. Send (2005), Objective analyses of hydrographic data for referencing profiling float salinities in highly variable environments, *Deep Sea Res., Part II*, *52*(3–4), 651–664, doi:10.1016/j.dsr2.2004.12.014.

Bushinsky, S. M., and S. Emerson (2013), A method for in-situ calibration of Aanderaa oxygen sensors on surface moorings, *Mar. Chem.*, *155*, 22–28, doi:10.1016/j.marchem.2013.05.001.

D'Asaro, E. A., and C. McNeil (2013), Calibration and stability of oxygen sensors on autonomous floats, *J. Atmos. Oceanic Technol.*, *30*, 1896–1906, doi:10.1175/JTECH-D-12–00222.1.

Edwards, B., D. Murphy, C. Janzen, and N. Larson (2010), Calibration, response, and hysteresis in deep-sea dissolved oxygen measurements, *J. Atmos. Oceanic Technol.*, *27*(5), 920–931, doi:10.1175/2009JTECHO693.1.

Emerson, S. R., C. Stump, and D. Nicholson (2008), Net biological oxygen production in the ocean: Remote in situ measurements of O2 and N2 in surface waters, *Global Biogeochem. Cycles*, *22*, GB3023, doi:10.1029/2007GB003095.

Fuenzalida, R., W. Schneider, J. Garcés-Vargas, L. Bravo, and C. Lange (2009), Vertical and horizontal extension of the oxygen minimum zone in the eastern South Pacific Ocean, *Deep Sea Res., Part II*, *56*(16), 992–1003, doi:10.1016/j.dsr2.2008.11.001.

Garcia, H. E., and L. I. Gordon (1992), Oxygen solubility in seawater: Better fitting equations, *Limnol. Oceanogr.*, *37*(6), 1307–1312.

Garcia, H. E., R. A. Locarnini, T. P. Boyer, J. I. Antonov, O. K. Baranova, M. M. Zweng, and D. R. Johnson (2010), *World Ocean Atlas 2009, Volume 3: Dissolved Oxygen, Apparent Oxygen Utilization, and Oxygen Saturation, NOAA Atlas NESDIS 70*, edited by S. Levitus U.S. Gov. Print. Off., Washington, D. C.

Gruber, N., S. C. Doney, S. R. Emerson, D. Gilbert, T. Kobayashi, A. Körtzinger, G. C. Johnson, K. S. Johnson, S. C. Riser, and O. Ulloa (2010), Adding oxygen to argo: Developing a global in situ observatory for ocean deoxygenation and biogeochemistry, *Proceedings of Ocean Obs '09: Sustained Ocean Observations and Information for Society*, Vol. 2, *ESA Publication WPP-306*, edited by J. Hall et al., doi:10.5270/OceanObs09.cwp.39.

Hamme, R. C., and S. R. Emerson (2006), Constraining bubble dynamics and mixing with dissolved gases: Implications for productivity measurements by oxygen mass balance, *J. Mar. Res.*, *64*(1), 73–95, doi:10.1357/002224006776412322.

Johnson, G. C., J. M. Toole, and N. G. Larson (2007), Sensor corrections for Sea-Bird SBE-41CP and SBE-41 CTDs*, *J. Atmos. Oceanic Technol.*, *24*(6), 1117–1130, doi:10.1175/JTECH2016.1.

Johnson, K. S., S. C. Riser, and D. M. Karl (2010), Nitrate supply from deep to near-surface waters of the North Pacific subtropical gyre, *Nature*, *465*(7301), 1062–1065, doi:10.1038/nature09170.

Johnson, K. S., L. J. Coletti, H. W. Jannasch, C. M. Sakamoto, D. D. Swift, and S. C. Riser (2013), Long-term nitrate measurements in the ocean using the in situ ultraviolet spectrophotometer: Sensor integration into the apex profiling float, *J. Atmos. Oceanic Technol.*, *30*, 1854–1866, doi:10.1175/JTECH-D-12–00221.1.

Juranek, L. W., R. A. Feely, D. Gilbert, H. Freeland, and L. A. Miller (2011), Real-time estimation of pH and aragonite saturation state from Argo profiling floats: Prospects for an autonomous carbon observing strategy, *Geophys. Res. Lett.*, *38*, L17603, doi:10.1029/2011GL048580.

Kihm, C., and A. Körtzinger (2010), Air-sea gas transfer velocity for oxygen derived from float data, *J. Geophys. Res.*, *115*, C12003, doi:10.1029/2009JC006077.

Kobayashi, T., T. Suga, and N. Shikama (2006), Negative bias of dissolved oxygen measurements by profiling floats, *Umi no kenkyu*, *15*(6), 479–498.

Körtzinger, A., J. Schimanski, and U. Send (2005), High quality oxygen measurements from profiling floats: A promising new technique, *J. Atmos. Oceanic Technol.*, *22*(3), 302–308.

Martz, T. R., K. S. Johnson, and S. C. Riser (2008), Ocean metabolism observed with oxygen sensors on profiling floats in the South Pacific, *Limnol. Oceanogr. Methods*, *53*(5–2), 2094–2111.

Najjar, R. G., and R. F. Keeling (1997), Analysis of the mean annual cycle of the dissolved oxygen anomaly in the World Ocean, *J. Mar. Res.*, *55*, 117–151.

Owens, W. B., and A. P. S. Wong (2009), An improved calibration method for the drift of the conductivity sensor on autonomous CTD profiling floats by θ–S climatology, *Deep Sea Res., Part I*, *56*(3), 450–457, doi:10.1016/j.dsr.2008.09.008.

Prakash, S., T. M. B. Nair, T. V. S. U. Bhaskar, P. Prakash, and D. Gilbert (2012), Oxycline variability in the central Arabian Sea: An Argo-oxygen study, *J. Sea Res.*, *71*, 1–8, doi:10.1016/j.seares.2012.03.003.

Riser, S. C. (2012), The use of dissolved oxygen sensors on profiling floats: Technical challenges and data quality, *Eos Trans. AGU*, *83*(4), Ocean Sci. Meet. Suppl., Abstract 11537.

Riser, S. C., and K. S. Johnson (2008), Net production of oxygen in the subtropical ocean, *Nature*, *451*(7176), 323–325, doi:10.1038/nature06441.

Stendardo, I., and N. Gruber (2012), Oxygen trends over five decades in the North Atlantic, *J. Geophys. Res.*, *117*, C11004, doi:10.1029/2012JC007909.

Tengberg, A., et al. (2006), Evaluation of a lifetime-based optode to measure oxygen in aquatic systems, *Limnol. Oceanogr. Methods*, *4*, 7–17.

Thierry, V., D. Gilbert, and T. Kobayashi (2011), Processing Argo OXYGEN data at the DAC level, Argo Project Office, Toulouse, France. [Available at http://www.argodatamgt.org/content/download/2928/21973/file/.]

Uchida, H., T. Kawano, I. Kaneko, and M. Fukasawa (2008), In situ calibration of optode-based oxygen sensors, *J. Atmos. Oceanic Technol.*, *25*(12), 2271–2281, doi:10.1175/2008JTECHO549.1.

Whitmire, A. L., R. M. Letelier, V. Villagran, and O. Ulloa (2009), Autonomous observations of in vivo fluorescence and particle backscattering in an oceanic oxygen minimum zone, *Opt. Express*, *17*(24), 21,992–22,004, doi:10.1117/12.190060.

Wong, A. P. S., G. C. Johnson, and W. B. Owens (2003), Delayed-mode calibration of autonomous CTD profiling float salinity data by θ – S climatology, *J. Atmos. Oceanic Technol.*, *20*(2), 308–318, doi:10.1175/1520-0426(2003)020<0308:DMCOAC>2.0.CO;2.

York, D. (1966), Least-squares fitting of a straight line, *Can. J. Phys.*, *44*, 1079–1086.